Collisional Quenching and Energy Transfer of the z5DJ o States of the Fe Atom

2 **AUTHORS**, INCLUDING:

Paul J Dagdigian
Johns Hopkins University
323 PUBLICATIONS **6,131** CITATIONS

Collisional Quenching and Energy Transfer of the $z^5D_J^o$ States of the Fe Atom

Boris Nizamov and Paul J. Dagdigian*

Department of Chemistry, The Johns Hopkins University, Baltimore, Maryland 21218-2685

Room-temperature thermal rate constants for quenching and energy transfer have been determined for the individual fine-structure levels of the $z^5D_J^o$ term of the Fe atom in collisions with He, Ar, and several molecular gases (N$_2$, O$_2$, H$_2$, and CH$_4$). The $z^5D_J^o$ term is the upper level of a transition at 372 nm which is convenient for laser fluorescence detection of the Fe atom. Emission profiles from all excited levels were observed to be exponential, and total removal rate constants were derived. The rate constants for the molecular gases were significantly larger [in the range of $(3-8) \times 10^{-10}$ molecule^{-1} cm^3 s^{-1}] than for the inert gases [$(0.3-1.3) \times 10^{-10}$ molecule^{-1} cm^3 s^{-1}]. No evidence for collisional transfer to the neighboring b^{3}H and a^{3}D states was found, and upper limits for the collisional transfer rate constants are reported. Rate constants for intramultiplet transfer within the $z^5D_J^o$ state were determined for He and O$_2$. The intramultiplet rate constants for He summed over all final fine-structure levels roughly equaled the total removal rate constants, while they were ~10% of the total removal constants for O$_2$.

1. Introduction

The collisional electronic quenching and energy transfer of electronically excited species is of both fundamental and practical importance. The availability of rate constants for these processes is particularly important in the use of laser diagnostic probes for determining concentrations of transient species in collisional environments (for example, flames).[1,2] The collisional behavior of excited transition metal atoms has been relatively unexplored. In this paper, we report a study of collisional quenching and energy transfer of the fine-structure levels of the Fe(z^5D^o) multiplet with a variety of collisional partners.

This work has been motivated by the need for collisional parameters of electronically excited Fe atoms in order to detect this species quantitatively in flames. Because of the ongoing phase-out of halons, including halogenated fire suppressants, there is a critical need for new, environmentally acceptable fire suppressants. However, an agent with all of the desirable properties is proving difficult to identify.[3] Some metal-containing compounds have been found to be considerably more effective flame inhibitors than are the halogen-containing compounds. In particular, Fe(CO)$_5$ has been found to be an especially strong inhibitor and at low concentrations very effectively reduces flame velocity.[4,5]

Unfortunately, the toxicity of Fe(CO)$_5$ prevents its use as a fire suppressant. Nevertheless, a detailed understanding of its effect upon flame chemistry would be very helpful in developing new fire suppressants. Kinetic modeling[6] of CH$_4$/air flames yields results similar to those observed in the laboratory and strongly suggests that inhibition by Fe(CO)$_5$ occurs primarily through a homogeneous mechanism involving reduction in the concentration of H atoms. Very recently, Skaggs et al.[7] reported the first measurements, in a low-pressure, nonpremixed flame, of a radical species (OH) as a function of added Fe(CO)$_5$. The present work was motivated by the desire also to measure the concentration of Fe-containing species, including the atom, in such flames.

Several different Fe atomic transitions out of the ground a^5D state have been employed for monitoring the time-dependent atomic concentration in low-pressure kinetics studies to determine thermal rate constants for reactions of the Fe atom with various molecular reagents. These include the $z^5D^o \leftarrow a^5D$ transition[8-10] and the $x^5F^o \leftarrow a^5D$ transition[11-14] at 372 and 248 nm, respectively. Goo et al.[15] have investigated the electronic quenching and collisional mixing among the z^3D^o and z^3F^o states, which are accessed from the ground state at 318−320 nm, in collisions with He and Ar. It should be noted that Fe atoms were prepared by multiphoton dissociation of Fe(CO)$_5$ and electronically excited with the same laser pulse. Hence, the translational energy of the Fe atoms was likely not thermally equilibrated.

From the point of view of laser diagnostic measurements of Fe atomic concentrations in flames, it is desirable to employ a transition with a relatively short radiative lifetime, but with relatively low excitation energy. In this way, the possibility of complicating collisional energy transfer processes to neighboring levels can be minimized. In the case of the z^3D^o and z^3F^o states, studied by Goo et al.,[15] pairs of fine-structure levels in each of these terms are very close in energy, and rapid collisional mixing was observed, leading to observed biexponential decays. It is interesting to note that the z^3D^o and z^3F^o states have the same electron configuration, 3d^{6}4s(a^4D)4p, and this may facilitate the collisional mixing. From the ground state, the longest-wavelength transition whose upper level has a sub-μs excited-state lifetime is the $z^5D^o \leftarrow a^5D$ multiplet at 372 nm.[16] This transition thus appears to be the most appropriate to employ for laser diagnostic measurements of the Fe atom. Accordingly, the electronic quenching and energy transfer of the $z^5D_J^o$ states in collisions with He, Ar, and several molecular gases are reported in this paper.

Figure 1 presents an energy-level diagram of the fine-structure levels of the Fe(z^5D^o) multiplet. This state has the electron configuration 3d^{6}4s(a^6D)4p. It can be seen from Figure 1 that the energy spacings between the fine-structure levels are comparable to or slightly larger than kT (208 cm^{-1}). In addition

---

* To whom correspondence should be addressed.
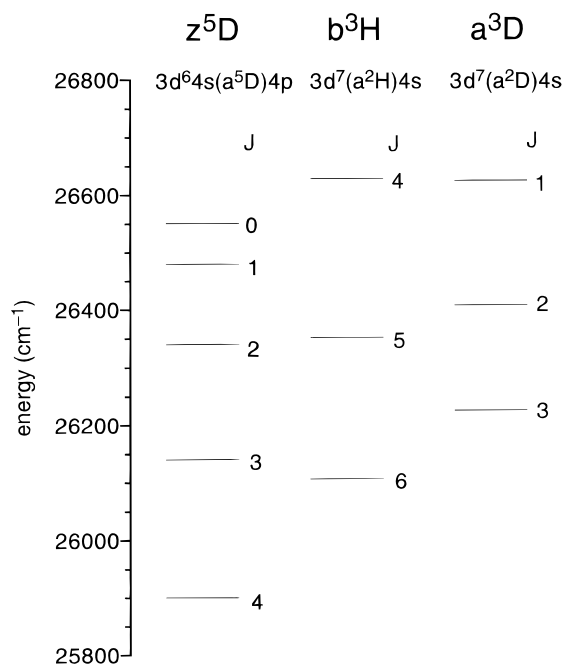
Figure 1. Energy-level diagram of the fine-structure levels of the z^5D^o, b^3H, and a^3D states of the Fe atom. The zero of energy is that of the ground a^5D_4 level.

to electronic quenching, the $z^5D_J{}^o$ levels can undergo collisional intramultiplet transfer. This process was studied in some detail for collisional transfer between the $n^2P_{1/2,3/2}{}^o$ fine-structure levels of alkali atoms.[17−21] Intramultiplet transfer has also been studied for multiplets of other classes of atoms with relatively small fine-structure splittings, including Ca(4s4p $^3P_J{}^o$),[22,23] Cr(3d^{5}4p $^7P_J{}^o$),[24] N(2p^{2}3p ^4D_J),[25] and Zn(4s4p $^3P_J{}^o$).[26] In the present experiment, intramultiplet transfer was observed by detection of emission from $z^5D_J{}^o$ levels other than the initially excited fine-structure level. Rate constants for intramultiplet transfer have been determined for several colliders and are compared with the total quenching rate constants.

In the same energy range as the z^5D^o state are the b^3H and a^3D states, which have the electron configurations 3d^7(a^2H)4s and 3d^7(a^2D)4s, respectively. For some pairs of levels, the energy gap between the $z^5D_J{}^o$ fine-structure levels and those of the b^3H and a^3D states is very small, e.g., 11 cm^{-1} in the case of the $z^5D_2{}^o$ and $b^3H_5{}^o$ levels (see Figure 1). It will be interesting to see whether collisional transfer between these levels having different electron configurations is facile.

2. Experimental Section

Iron atoms were produced by photolysis[27−29] of Fe(CO)$_5$ at 193 nm. Photolysis was carried out in a cell consisting of a central chamber with opposing sidearms for entry and exit of the photolysis and probe laser beams. Iron pentacarbonyl precursor was premixed with He in a 10-L bulb; the Fe(CO)$_5$ partial pressure was equal to or less than its room-temperature vapor pressure (36 Torr), and the He partial pressure was 200−500 Torr. The mixture was admitted into the central chamber about 15 cm upstream from the observation zone. The quencher gas was introduced through the ends of the sidearms and the gas mixture was slowly flowed through the cell. The total pressure was in the range 0.3−20 Torr depending on the experiment, while the partial pressure of the Fe(CO)$_5$/He mixture was 20 mTorr. The purity of the He, Ar, H$_2$, and N$_2$ reagents was better than 99.997%, and the purities of CH$_4$ and O$_2$

employed were 99.99% and 99.6%, respectively. The absolute pressure was monitored with a capacitance manometer (MKS).

The 193-nm output of a LEXTRA 100 (Lambda Physik) ArF excimer laser was focused using a 1-m lens above the slit of a 1-m f/9 Fastie-Ebert spectrometer with 8 Å/mm dispersion in the first order. The spectrometer was operated at a spectral resolution of 4 Å. The typical pulse energy of the excimer laser in the vacuum chamber was ∼40 mJ. The probe laser beam (∼4 mm in diameter) was introduced through the opposite sidearm and had spectral full width at half-maximum (fwhm) of 0.2 cm^{-1} and temporal fwhm of 8 ns. The energy of the probe laser (∼100 μJ) was adjusted so that the probed transitions were saturated. The delay (controlled by a digital delay generator) between the photolysis and the probe lasers was 10 μs. This time is sufficient for most of the emission from photolytically generated excited states to decay away, but short enough so that significant population remains in all the fine-structure levels of the a^5D_J ground state. The delay between the photolysis and excitation lasers is long enough to allow thermalization of the Fe atoms to a room-temperature velocity distribution.

Fluorescence was detected with two separate photomultiplier (PMT) detectors. One PMT was placed at the exit slit of the spectrometer and was used to monitor emission from a selected $z^5D_J{}^o$ level of the upper state when waveforms were measured or wavelength-resolved fluorescence excitation spectra were recorded. The second PMT was used to monitor the total fluorescence signal from the excited upper-state level. The latter detector allowed us to check for variations in the concentration of Fe atoms due to changes in the partial pressure of the Fe-(CO)$_5$ precursor and/or the 193-nm laser energy. The $J = 0−4$ levels of the $z^5D_J{}^o$ state were excited from the ground a^5D_J state using the $J' \leftarrow J'' = 0−1$, 1−2, 2−3, 3−3, and 4−4 lines (385.5−389.6 nm wavelength range), and populations in these levels were monitored by observing emission in the same lines.

The transient signals from the PMTs were directed to gated integrators (Stanford Research Systems SR250), and their outputs were collected under computer control and stored on magnetic media for later analysis. The waveforms were collected using the 600 MHz input of a Lecroy 9360 digital oscilloscope (1 G sample/s) and were stored on magnetic media for later analysis.

3. Results

3.1. Total Removal Rate Constants. Waveforms of the fluorescence decay from the $z^5D_J{}^o$ levels, for $J = 0−4$, were recorded at different pressures of He, Ar, N$_2$, O$_2$, H$_2$, and CH$_4$. The pressure range for each quenching gas was chosen so that the first-order decay constant would increase by approximately a factor of 2 over the purely radiative decay rate in the pressure range studied. For all levels and quenching gases, the semilogarithmic plots of the waveforms were observed to be linear to within the experimental uncertainties over the first three to four decay lifetimes, and the decays thus appeared to be single-exponential. An example of a waveform is given in Figure 2.

Waveforms of the time-dependent emission from the laser-excited $z^5D_J{}^o$ levels were fit over the first three decay times starting ∼40 ns after the laser pulse. About 20−30 points were used for each Stern−Volmer (SV) plot, from which total quenching rate constants and radiative lifetimes were determined. Sample SV plots for the $J = 0$ level are shown in Figure 3. Total quenching rate constants are summarized in Table 1. The radiative lifetimes for the $J = 0$, 1, 2, 3, and 4 levels were

Quenching and Energy Transfer of the Fe Atom

J. Phys. Chem. A, Vol. 104, No. 27, 2000 **6347**

TABLE 1: Total Collisional Removal Rate Constants (Units: 10^{-10} molecule^{-1} cm^3 s^{-1}) for the Fine-Structure Levels J of the Fe z^5D^o State

collider	$J = 0$	$J = 1$	$J = 2$	$J = 3$	$J = 4$
He	0.48 ± 0.04	0.96 ± 0.06	0.56 ± 0.04	0.26 ± 0.02	0.36 ± 0.02
Ar	0.37 ± 0.04	0.47 ± 0.02	0.77 ± 0.04	0.72 ± 0.04	1.35 ± 0.08
N_2	2.71 ± 0.24	3.18 ± 0.30	3.64 ± 0.52	3.61 ± 0.24	3.82 ± 0.24
O_2	3.49 ± 0.26	3.65 ± 0.22	4.56 ± 0.40	4.56 ± 0.34	4.43 ± 0.30
H_2	6.38 ± 0.40	7.34 ± 0.48	8.33 ± 0.60	7.92 ± 0.56	8.28 ± 0.58
CH_4	4.93 ± 0.40	6.25 ± 0.54	5.20 ± 0.68	4.94 ± 0.32	4.15 ± 0.32
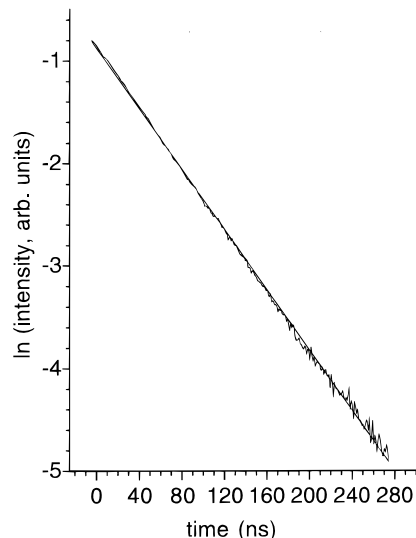
Figure 2. A semilogarithmic plot of fluorescence decay from the $z^5D_1^o$ state collected at 1.08 Torr of He. The straight line is a least-squares fit to the decay, as described in the text.
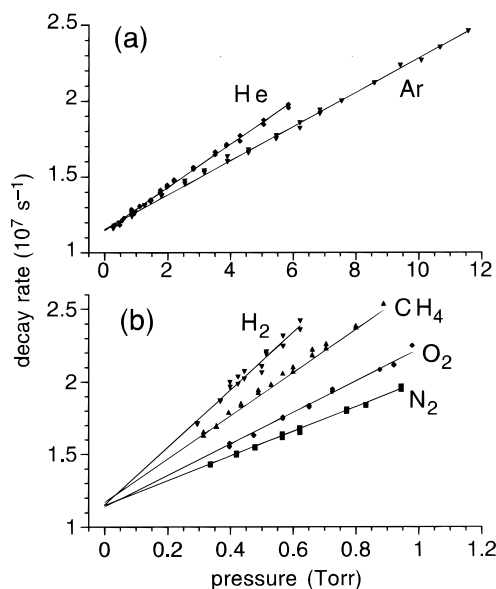
Figure 3. Stern–Volmer plots of the decay rates as a function of collider gas pressure for the $z^5D_0^o$ state of the Fe atom for (a) atomic and (b) molecular colliders.

determined to be equal to 87.7 ± 0.8, 84 ± 3, 85.4 ± 1.4, 85.8 ± 0.8, and 84.5 ± 0.7 ns, respectively, from the zero-pressure intercepts of the SV plots. These values are in good agreement with the results of previous measurements.[30]

The observed purely exponential decays suggest that collisional transfer to the closely lying fine-structure levels of the b^3H and a^3D levels is small. Otherwise, biexponential decays, involving rapid equilibration of the coupled, nearly isoenergetic levels (e.g., $z^5D_2^o$ and b^3H_5, see Figure 1) and then slower

relaxation of this coupled system, would be observed. Single-exponential decay was even observed for the $z^5D_2^o$, for which the $b^3H_5^o$ state lies extremely close in energy, as discussed above.

Kinetic modeling was carried out to estimate upper bounds for the collisional transfer rate constants to the b^3H and a^3D states. The following two-state model was employed:

$$dN_1/dt = -(k_1^{rad} + k_1^{tot} n)N_1 + k_{21}nN_2 \qquad (1)$$

$$dN_2/dt = k_{12}nN_1 - (k_2^{rad} + k_2^{tot} n)N_2 \qquad (2)$$

Here, N_1 is the concentration of the initially excited $z^5D_J^o$ level, N_2 is the concentration of level(s) in the b^3H and a^3D states, k_i^{rad} is the radiative decay rate of level i, k_i^{tot} is the bimolecular total removal rate constant, k_{ij} is the bimolecular rate constant from collisional transfer from level i to level j, and n is the density of the collision partner. It is to be noted that k_i^{tot} encompasses all collisional removal processes, including quenching and energy transfer. Radiative decay of the b^3H and a^3D states can be neglected because these states have only $\Delta S \neq 0$ transitions in the infrared. Because the radiative decay rate of the $z^5D_J^o$ levels is relatively large, deviations from linear behavior in the semilogarithmic plots due to energy transfer into the b^3H and a^3D states could be undetected if the rate constants (k_{12} in eq 1) were small. In this case, the second, slower component of the biexponential decay may be undetected within the signal-to-noise ratio (S/N) of the $z^5D_J^o$ emission decay profile.

With our dynamical range, the fluorescence signal could be followed over approximately five decay lifetimes. The sensitivity to the energy transfer process is greatest at the highest pressures, where the collisional removal rate becomes comparable to the radiative decay rate. Considering the case of the $z^5D_2^o$ and b^3H_5 states, for which the energy gap is very small, we conclude from integration of eqs 1 and 2 that we could detect transfer between these states if the $z^5D_2^o \rightarrow b^3H_5$ transfer rate constant $k(z^5D_2^o \rightarrow b^3H_5)$ were > 0.4 times the $z^5D_2^o$ total removal rate constant, if it is assumed that the bimolecular total removal rate constant for the b^3H_5 state were the same as for the $z^5D_2^o$ state. Our sensitivity to detection of energy transfer would be greater if the bimolecular total removal rate constant of the b^3H_5 state were small. In this case, it would be possible to detect collisional transfer if $k(z^5D_2^o \rightarrow b^3H_5) > 0.2 \, k^{tot}(z^5D_2^o)$. It was not possible to detect collisional transfer to the b^3H and a^3D states by observing emission from the final states, because fluorescence from these levels occurs in the infrared and would not be detectable in this apparatus and because the radiative decay rates are expected to be small.

3.2. Intramultiplet Relaxation in He and O_2. Although collisional transfer to the b^3H and a^3D states was not detected, we did observe collision-induced emission from fine-structure levels other than the initially excited level within the z^5D^o state. Rate constants $k(J_i \rightarrow J_f)$ for collisional transfer between fine-structure levels of the z^5D^o multiplet were measured for two of
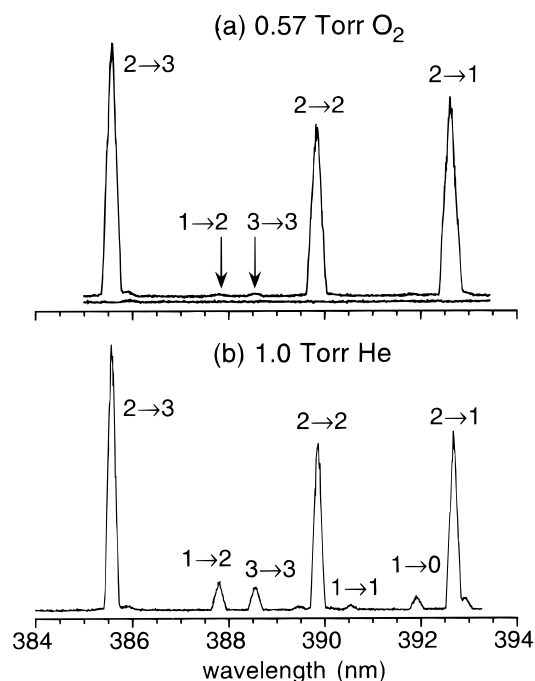
Figure 4. Emission spectra in the $z^5D_J^o \rightarrow a^5D_{J''}$ multiplet following excitation of the $z^5D_2^o$ state in the presence of (a) 0.57 Torr O_2 and (b) 1.0 Torr He. The upper- and lower-state total angular momenta of each line are denoted as $J - J''$. The detection time gates were 0−400 ns and 0−500 ns for the spectra in panels (a) and (b), respectively.

the colliders by recording emission spectra in the 384−394 nm wavelength range following excitation of one of the $z^5D_J^o$ levels. For He as a buffer gas, spectra were collected at 0.5 and 1.0 Torr, while spectra for O_2 were collected at 0.57 Torr. The signal was observed in time windows of 0−500 ns for He and 0−400 ns for O_2. These time windows are sufficiently long that essentially the whole fluorescence decays curves were sampled. Sample experimental spectra are shown in Figure 4.

For all initial states, the $\Delta J = \pm 1$ collision-induced transitions were observed, while $\Delta J = +2$ transitions were also observed for the $J = 0$ and 1 initial levels. The two-state kinetic model in eqs 1 and 2 was used to analyze the data. In this case, the radiative decay rate constants of the initial and final levels are approximately equal. For the conditions of our experiment, $k_{12} n/k_1' \ll 1$, where the first-order total decay rate constant of the initial level is denoted as $k_1' = k_1^{rad} + k_1^{tot} n$. If collisional transfer between different final levels can be neglected and the total decay rate constants of the initial and final levels are equal, i.e., $k_1' = k_2' \equiv k'$, then it can be easily shown that

$$I_1/I_2 = k_{12}\, n/k' \tag{3}$$

where I_1/I_2 is a ratio of the time-integrated populations, which can be calculated from the ratio of intensities. In our calculations, the value of k_1' was taken from the corresponding SV plot. Einstein coefficients from the NIST database[16] were used to convert ratios of intensities to ratios of populations.

Waveforms, showing transfer of population from the $J = 1$ level to $J = 2$ at 0.93 Torr He, are shown in Figure 5. These waveforms demonstrate that population transfer occurs directly and that no intermediate state is involved. Similar waveforms were observed for other intramultiplet transitions. For our conditions, for which $k_1' = k_2'$ and the reverse process can be neglected, the shape of the waveform for emission from level 2 is relatively insensitive to the value of k_{12}. In this case, the
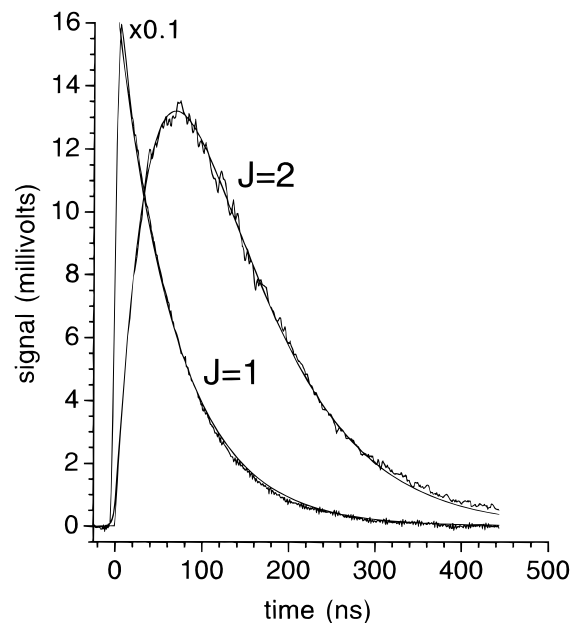
Figure 5. Waveforms of the emission from the $z^5D_J^o$ states for $J = 1$ and 2 with laser excitation of the $z^5D_1^o$ state, showing transfer of population from the $z^5D_1^o$ level to the $z^5D_2^o$ level. These waveforms were collected at 0.93 Torr He. The smooth curves represent fits to the waveforms (exponential decay and eq 4).

time-dependent population of the final level is given by

$$N_2 = N_1^o\, k_{12}\, n\, t\, \exp(-k_1'\, t) \tag{4}$$

where N_1^o is the initial population of the parent level. As shown in Figure 5, eq 4 provides a good representation of the time-dependent population of the final levels. Values for the transfer rate constants were obtained from the relative intensities in the emission spectra, through eq 3.

To check the validity of the assumption that indirect transfer between the initial and final levels can be neglected for the conditions of our experiment, emission spectra with He as a buffer gas were collected at two pressures, 0.5 and 1.0 Torr. For each pressure and initial J level, two to three scans were recorded. Within experimental error, the derived bimolecular transfer rate constants were independent of the pressure of the buffer gas. This provides confidence that our assumption was valid.

Transfer rate constants, obtained using this approach, are summarized in Table 2. For one pair of levels ($J = 1$ and 2), the forward and reverse transfer rate constants, $k(1 \rightarrow 2)$ and $k(2 \rightarrow 1)$, could be independently measured. This ratio of these rate constants equals 3.3 ± 0.4 and is in good agreement with the ratio (3.1) predicted by detailed balance. In Table 2, we have also included estimates for the sum of the rate constants for all intramultiplet transitions out of each fine-structure level except the lowest-energy level ($J = 4$). Unmeasured endothermic rate constants were estimated from the rate constants for the corresponding exothermic transitions, when the latter were available.

4. Discussion

The total removal rate constants are of significant magnitude for all colliders studied. However, the rate constants for He and Ar are roughly an order of magnitude smaller than those of the molecular colliders. Goo et al.[15] reported apparent quenching rate constants for the z^3D^o and z^3F^o states with He and Ar colliders. These states lie approximately 6000 cm^{-1} higher in

Quenching and Energy Transfer of the Fe Atom

J. Phys. Chem. A, Vol. 104, No. 27, 2000 **6349**

TABLE 2: Rate Constants (Units, 10^{-11} molecule^{-1} cm^3 s^{-1}) for Collisional Transfer between the Fine-Structure Levels J of the Fe z^5D^o State

initial J	final J	$k(J_i \rightarrow J_f)$ (He)	$k(J_i \rightarrow J_f)$ (O$_2$)
0	1	1.71 ± 0.16	3.5 ± 1.1
	2	3.15 ± 0.61	0.8 ± 0.2
	sum^a	$\geq 4.86 \pm 0.64$	$\geq 4.3 \pm 1.1$
1	2	9.1 ± 1.8	3.1 ± 0.9
	3	1.71 ± 0.22	0.9 ± 0.3
	sum^a	$\geq 10.8 \pm 1.8$	$\geq 4.0 \pm 1.0$
2	3	2.54 ± 0.16	0.6 ± 0.2
	1	2.80 ± 0.28	
	sum^a	$\geq 5.34 \pm 0.32$	$\geq 1.5 \pm 0.4$
3	4	0.56 ± 0.06	0.7 ± 0.2
	sum^a	$\geq 1.13 \pm 0.10$	$\geq 0.85 \pm 0.2$
4	sum^a	$\geq 0.14 \pm 0.02$	$\geq 0.2 \pm 0.06$

^{a} Sum of rate constants to all final fine-structure levels within Fe(z^5D^o). Unmeasured rate constants for endothermic processes were calculated by detailed balance from the corresponding exothermic rate constants, where available.

energy than those studied here, and their relaxation kinetics were complicated by strong collisional-state mixing. The apparent quenching rate constants they derived for these states ($2.0-3.6 \times 10^{-10}$ molecule^{-1} cm^3 s^{-1} for He and $0.7-1.8 \times 10^{-10}$ molecule^{-1} cm^3 s^{-1} for Ar) are significantly larger than those reported here.

For He, our total removal rate constants can be compared to the rate constants for intramultiplet relaxation to other fine-structure levels of the $z^5D_J^o$ multiplet. Sums of the intramultiplet relaxation rate constants to all final fine-structure levels for each initial level J are presented in Table 2. Comparison of these rate constants with the total removal rate constants in Table 1 shows that essentially all the collisional transfer out of the $J = 0-2$ levels is through fine-structure changing collisions within the multiplet. This finding suggests that the upper bound for collisional transfer to the b^3H and a^3D states reported in the previous section is a considerable overestimate of the transfer rate for these fine-structure levels in collisions with He. For the lower-energy $J = 3$ and 4 levels, fine-structure changing transitions comprise ~40% of the total removal rate constant.

We see from Tables 1 and 2 that the total rate constant for fine-structure changing transitions in collisions with He depends significantly upon the initial level J. The largest total rate constant is for the $J = 1$ level, whereas the smallest are for the lower-energy $J = 3$ and 4 levels. The probability of Fe(z^5D^o)–He collision-induced fine-structure changing transitions is substantial. Dividing by the average relative velocity, the total removal rate constant for the $J = 1$ level corresponds to a cross section of 7.4 Å^2.

The mechanism for collision-induced fine-structure transitions has been considered in detail previously for collisions of excited n^2P^o alkali and $nsnp$ $^3P^o$ alkaline earth atoms.[21,23] This is a nonadiabatic process that occurs near internuclear separations for which the fine-structure splitting equals the energy separation between the electrostatic potential energy curves (Π and Σ states for the alkali and alkaline earth states mentioned above).

The mechanism for collision-induced fine-structure-changing transitions in atomic states of high spin multiplicity and orbital angular momentum [$S = 2$ and $L = 2$ for the Fe(z^5D^o) state] is considerably more complicated, given that there are a number of possible transitions among the fine-structure levels. The magnitude of the rate constants is dependent upon both the energy gap between the initial and final levels and the degree of nonadiabatic coupling. It can be seen in Figure 1 that the energy gaps are larger between the levels of lower energy (from

the Landé interval). (It should be noted that the fine-structure $z^5D_J^o$ levels are inverted.) This provides an explanation for the smaller rate constants out of the $J = 3$ and 4 initial levels.

The approach of the collider causes a lifting of the degeneracy of a given Fe fine-structure level, and each level J splits into a set of molecular curves with $\Omega = 0 - J$. The coupling of these curves correlating with different asymptotic fine-structure levels is responsible for the collision-induced fine-structure changes. This coupling can be due either to nonadiabatic terms of the radial kinetic energy ($\Delta\Omega = 0$) or to Coriolis coupling ($\Delta\Omega = \pm 1$). We see in Table 2 that the $k(0 \rightarrow 1)$ rate constant is significantly smaller than $k(0 \rightarrow 2)$, despite the fact that energy gap for the latter transition is larger. As pointed out by Alexander et al.[23] for the Ca($^3P^o$)–He system, there is no radial coupling of the $\Omega = 0$ curves for $J = 0$ and 1. Similarly, there is no radial coupling between these curves for collisions of Fe(z^5D^o) because the case (c) $\Omega = 0$ states correlating with the $J = 0$ and 1 asymptotes have opposite reflection symmetry, whereas there is direct radial coupling between the $\Omega = 0$ states of $J = 0$ and 2.

Electrostatic potential energy curves are not available for the interaction of Fe(z^5D^o) and Ar. However, Partridge and Bauschlicher[31] have calculated such curves for the interaction of the ionic core of this state, Fe$^+$($3d^64s$ a^6D), with Ar. The energetic ordering of the molecular Fe$^+$–Ar electronic curve was rationalized by the electron occupancy of the $3d\sigma$, $3d\pi$, and $3d\delta$ orbitals. We expect that the ordering of the $^5\Delta$, $^5\Pi$, and $^5\Sigma$ states arising from the Fe(z^5D^o) + Ar asymptote will depend primarily on the $4p\pi/4p\sigma$ character of these states. These curves are required for the calculation of the Ω-dependent potential energy curves, which are eigenvalues of the electrostatic + spin–orbit Hamiltonian and the quantum state-to-state cross sections.

The cross sections for collision-induced intramultiplet transfer in Fe(z^5D^o)–O$_2$ collisions are comparable to those for collisions with He. For example, the lower limit quoted in Table 2 for the total rate constant for intramultiplet transfer out of the $J = 1$ level in O$_2$ collisions is 7.2 Å^2, which is quite close in magnitude to the cross section quoted above for He. However, in contrast to the situation for He, the intramultiplet transfer for O$_2$ constitutes only $\leq 10\%$ of the total removal rate constants quoted in Table 1. Unlike the inert gas colliders, collisions with O$_2$ can also be reactive. The energetics of the Fe + O$_2$ → FeO + O reaction are such that excited FeO states can, in principle, be produced in this reaction. This reaction is significantly endothermic ($\Delta H_0^o = +91 \pm 8$ kJ mol^{-1}), and ground-state Fe atoms react only in termolecular fashion to form FeO$_2$.[12] However, reaction of the Fe(z^5D^o) state is 224 kJ mol^{-1} exothermic, and formation of FeO states emitting in the visible (D$^5\Delta$, C$^5\Pi$, and B$^5\Phi$)[32] is energetically allowed. Spectral scans were taken to search for emission from excited FeO product states, but none was found. This implies that reactive quenching to form emitting FeO states is negligible. However, formation of ground-state FeO and/or low-lying states in the quenching of Fe(z^5D^o) by reaction with O$_2$ is not ruled out. Chemical reaction is also allowed for reaction of Fe(z^5D^o) with H$_2$ and CH$_4$ colliders. However, the small FeH bond energy (D$_0 = 157 \pm 8$ kJ mol^{-1})[33] precludes formation of emitting FeH states.

It can be seen in Table 1 that the total removal rate constants for all the molecular colliders are substantially larger than those of the inert gases, regardless of whether chemical reaction is allowed (O$_2$, H$_2$, CH$_4$) or not (N$_2$). With the assumption of velocity-independent cross sections, the rate constants reported in Table 1 for the $J = 4$ level correspond to cross sections of

66, 80, 46, and 58 $Å^2$ for the N_2, O_2, H_2, and CH_4 colliders, respectively. The variation of the total removal rate constants as a function of the total angular momentum J is smaller for the molecular colliders than for the inert gases. This indicates that collisional removal for the molecular colliders is less governed by the specific couplings to the individual fine-structure levels, as in the case of the inert gases.

The final point worthy of comment is the lack of evidence for collisional transfer to the neighboring b^3H and a^3D states, although our derived upper bounds on the energy transfer rate constants are liberal. Our observations stand in sharp contrast to the observations of Goo et al.,[15] who observed rapid collisional coupling of the z^3D^o and z^3F^o states. In this case, the two states possess the same electron configuration [$3d^64s$-(a^4D)$4p$], but with different coupling of the outer $4p$ electron with the core to yield different values of the total orbital angular momentum. For the z^5D^o state under study here, the electron configurations of the neighboring b^3H and a^3D states differ from that of the z^5D^o state by two electrons. This finding suggests that the matrix elements coupling the initial and final states are small, consistent with the unobserved collisional transfer.

References and Notes

(1) Eckbreth, A. C. *Laser Diagnostics for Combustion Temperature and Species Measurements*; Abacus Press: Tunbridge Wells, U.K., 1988.

(2) Kohse-Höinghaus, K. *Prog. Energy Combust. Sci.* **1994**, *20*, 203.

(3) *Halon Replacements: Technology and Science*; Miziolek, A. W., Tsang, W., Eds.; ACS Symposium Series 611; American Chemical Society: Washington, DC, 1995.

(4) Bonne, U.; Jost, W.; Wagner, H. G. *Fire Res. Abstracts Rev.* **1962**, *4*, 6.

(5) Reinelt, D.; Linteris, G. T. *Twenty-Sixth Symposium (International) on Combustion*; The Combustion Institute: Pittsburgh, 1996; p 432.

(6) Rumminger, M. D.; Reinelt, D.; Babushok, V.; Linteris, G. T. *Combust. Flame* **1999**, *116*, 207.

(7) Skaggs, R. R.; McNesby, K. L.; Daniel, R. G.; Homan, B.; Miziolek, A. W. *Combust. Sci. Technol.*, in press.

(8) Campbell, M. L.; Metzger, J. R. *Chem. Phys. Lett.* **1996**, *253*, 158.

(9) Mitchell, S. A.; Hackett, P. A. *J. Chem. Phys.* **1990**, *93*, 7822.

(10) Fontijn, A.; Kursius, S. C. *Chem. Phys. Lett.* **1972**, *13*, 507.

(11) Helmer, M.; Plane, J. M. C. *J. Chem. Soc., Faraday Trans.* **1994**, *90*, 31.

(12) Helmer, M.; Plane, J. M. C. *J. Chem. Soc., Faraday Trans.* **1994**, *90*, 395.

(13) Plane, J. M. C. *J. Chem. Soc., Faraday Trans.* **1996**, *92*, 4371.

(14) Plane, J. M. C.; Rollason, R. J. *Phys. Chem. Chem. Phys.* **1999**, *1*, 1843.

(15) Goo, J. S.; Lee, K.; Bae, S. C.; Ku, J. K. *J. Chem. Phys.* **1996**, *105*, 7485.

(16) Fuhr, J. R.; Martin, G. A.; Wiese, W. L. *J. Phys. Chem. Ref. Data* **1988**, *17*, Suppl. 4.

(17) Lemoine, D.; Robbe, J. M.; Pouilly, B. *J. Phys. B* **1988**, *21*, 1007.

(18) Mestdagh, J. M.; de Pujo, P.; Pascale, J.; Cuvellier, J.; Berlande, J. *Phys. Rev. A* **1987**, *35*, 1043.

(19) Düren, R.; Hasselbrink, K.; Hillrichs, G. *J. Chem. Phys.* **1988**, *89*, 2822.

(20) Anderson, R. W.; Goddard, T. P.; Parravano, C.; Warner, J. *J. Chem. Phys.* **1976**, *64*, 4037.

(21) Nikitin, E. E. *Adv. Chem. Phys.* **1975**, *28*, 317.

(22) Yuh, H.-J.; Dagdigian, P. J. *Phys. Rev. A* **1983**, *28*, 63.

(23) Alexander, M. H.; Orlikowski, T.; Straub, J. E. *Phys. Rev. A* **1983**, *28*, 73.

(24) Parson, J. M.; Ishikawa, T. *J. Chem. Phys.* **1984**, *80*, 3137.

(25) Jeffries, J. B.; Copeland, R. A.; Crosley, D. R. *J. Chem. Phys.* **1989**, *91*, 2200.

(26) Umemoto, H.; Masaki, A.; Ohnuma, T.; Misiazu, F.; Fuke, F. *J. Phys. B* **1991**, *24*, 1639.

(27) Waller, I. M.; Hepburn, J. W. *J. Chem. Phys.* **1988**, *88*, 6658.

(28) Lee, K.; Goo, H. S.; Ku, J. K. *Chem. Phys. Lett.* **1996**, *262*, 610.

(29) Bañares, L.; Baumert, T.; Bergt, M.; Kiefer, B.; Gerber, G. *J. Chem. Phys.* **1998**, *108*, 5799.

(30) Engelke, D.; Bard, A.; Kock, M. *Z. Phys. D* **1993**, *27*, 325.

(31) Partridge, H.; Bauschlicher, C. W., Jr. *J. Phys. Chem.* **1994**, *98*, 2301.

(32) Merer, A. J. *Annu. Rev. Phys. Chem.* **1989**, *40*, 407.

(33) Schultz, R. H.; Armentrout, P. B. *J. Chem. Phys.* **1991**, *94*, 2262.